Vol. 36, No. 4 (2014) 361-374

Tribology in Industry

www.tribology.fink.rs

RESEARCH

Wear Micro-Mechanisms of Composite WC-Co/Cr - NiCrFeBSiC Coatings. Part I: Dry Sliding

D. Kekes[a], P. Psyllaki[a], M. Vardavoulias[b]

[a]*Department of Mechanical Engineering, Technological Education Institute (TEI) of Piraeus, 250 Thivon Avenue and P. Ralli, 122 44, Egaleo, Greece,*
[b]*PyroGenesis SA, Technological Park of Lavrion, 195 00 Lavrion, Greece.*

Keywords:

Composite coatings
CerMet
HVOF deposition
Sliding friction
Wear micro-mechanisms

Corresponding author:

P. Psyllaki
Department of Mechanical Engineering, Technological Education Institute (TEI) of Piraeus, 250 Thivon Avenue and P. Ralli, 122 44, Egaleo, Greece
E-mail: psyllaki@teipir.gr

A B S T R A C T

The influence of the cermet fraction in cermet/ metal composite coatings developed by High-Velocity Oxyfuel Flame (HVOF) spraying on their tribological behaviour was studied. Five series of coatings, each one containing different proportion of cermet-metal components, prepared by premixing commercially available feedstocks of NiCrFeBSiC metallic and WC-Co/Cr cermet powders were deposited on AISI 304 stainless steel substrate. The microstructure of as-sprayed coatings was characterized by partial decomposition of the WC particles, lamellar morphology and micro-porosity among the solidified splats. Tribological behavior was studied under sliding friction conditions using a Si_3N_4 ball as counterbody and the friction coefficient and volume loss were determined as a function of the cermet fraction. Microscopic examinations of the wear tracks and relevant cross sections identified the wear mechanisms involved. Coatings containing only the metallic phase were worn out through a combination of ploughing, micro-cracking and splat exfoliation, whilst those containing only the cermet phase primarily by micro-cracking at the individual splat scale. The wear mechanisms of the composite coatings were strongly affected by their randomly stratified structure. In-depth cracks almost perpendicular to the coating/ substrate interface occurring at the wear track boundaries resulted in cermet trans-splat fracture.

1. INTRODUCTION

The term "cemented carbides" is used to describe a subgroup of cermets, where a ceramic phase of hard carbide particles, such as WC, TiC, Cr_3C_2, etc., in percentages of the order of 80-90 %, is bound together by a metal binder phase, typically Co, Ni, Mo or a mixture of them. Their high hardness and wear resistance under unlubricated conditions induced by the ceramic phase has established them as the materials of choice in applications under harsh conditions, like hard metal cutting, rock drilling, etc [1].

Their excellent properties as sintered monolithic anti-wear components have rendered cermets

also attractive as coatings of metallic parts of tribosystems operating under sliding, abrasion and erosion conditions under high temperature and corrosive atmospheres [2]. Thermal spraying is the principal deposition technique to obtain such coatings, with thickness in the range of 200-400 μm. However, the main drawbacks of thermal-sprayed coatings were their high porosity [3], common characteristic of all ceramic coatings elaborated by thermal spraying, and especially in the case of carbide cermets, the decarburization/ dissociation of the carbide particles due to the high temperatures developed during deposition. The issue of high porosity was tackled in a satisfactory way in the one hand by applying High Velocity Oxy-Fuel (HVOF) spraying and in the other hand by employing powder feedstocks of sub-micron and nano-size [4-8]. In HVOF spraying, oxygen and fuel gas are mixed and burnt in a combustion chamber at high flow-rates and pressures up to 12 bar, producing a high-speed jet. Feedstock particles are accelerated with high velocities and relatively low temperature compared to other thermal spray processes such as atmospheric or vacuum plasma spraying. The coatings obtained exhibit high density and superior bond strength to the metallic substrate [9,10]. The industrially relevant potential of HVOF has been demonstrated by the development of not only coatings but also for the spray-forming of free-standing, solid, carbide-based components of varying thickness [11]. Recently, HVAF and LPG-fueled HVOF, where oxygen was replaced by compressed air [12-14] and fuel gas by LPG [15], respectively, were proposed as alternatives to the traditional HVOF technique. Despite the lower temperature developed in HVOF, the second drawback mentioned above, i.e. carbide decarburization, is not completely eliminated. In fact, the use of nano-size powder feedstocks favors carbide particles decomposition due to the inherent higher surface area-to-volume ratio of carbide grains in such powders [8].

HVOF is particularly suitable for the deposition of WC-based cermet HVOF coatings, since is designed to retain a larger fraction of WC in the coating. The hypersonic velocity of the flame shortens the powder-flame interaction time and together with lower flame temperature limit WC decomposition [16]. However, its decomposition to substoichiometric W_2C and metallic W and the WC reaction with the metal binder to η-phase Me-W-C, both deteriorating the coatings hardness values and consequently their anti-wear performance, have been frequently reported [2,16-24]. Recent studies, addressing this issue are focused on the optimization of the deposition process parameters (e.g. spray distance, oxygen and flue flow rates) via Taguchi analysis using as a criterion the coating hardness values achieved [25,26]

Studies on the tribological performance of WC-based cermets concern abrasion, sliding friction and fretting wear testing [4,5,8-10,12,15,19,21-28] according to the ASTM G65, G99 and D6037 specifications, respectively. Relevant research findings demonstrated high wear resistance comparable to that of sintered cermets [9]; thus these coatings are the most widely considered as being capable of replacing hard chromium electrodeposits on a variety of industrial components, especially in automotive applications [3,15,27]. Such coatings often operate in corrosive environments, where the chemical passivity of the metal binder is a demand to avoid coatings total failure through electrochemical reactions or pitting. Relevant works concern the comparative study of influence of various types of binders, as Ni, Co, or Ni-Cr, Co-Cr mixtures [4,5,13,17] in percentages lower than 20 %, on the anti-corrosive resistance of WC-based cermet coatings, each one inhibiting different corrosion type. Especially, alloys of the Ni-Cr system exhibit excellent corrosion resistance in aqueous environment, as well as high temperature wear resistance and can be directly deposited as dense and well-adhered coatings onto steel substrates by HVOF spraying [29-33].

In order to exploit the beneficial presence of a deformable phase in achieving enhanced damage tolerance of anti-wear carbide-based coatings, recent studies are focused on the behavior of composite cermet / metal coatings, in which the metallic phase participates not as binder metal, but as a distinct matrix of the product in percentages higher than 20 %. Various such composite coatings systems have been studied. Particular examples include functionally graded WC-Co/ NiAl HVOF coatings exhibiting better ductility and toughness conferred by the metallic splats to the cermet systems [34], as well as composite WC-Co/ NiCrFeSiB coatings deposited from mechanically

alloyed feedstock powders to enhance homogeneity of cermet dispersion in the ductile metallic phase [35].

The objective of this study was to evaluate the wear micro-mechanisms taking place during surface mechanical loading of ceramic-metal, randomly stratified coatings. In this perspective, two representative wear tests were selected, namely sliding and cavitation erosion. Composite HVOF coatings were deposited onto stainless steel substrate, by premixing WC-Co/Cr and NiCrFeBSiC commercial powders in various percentages. The present, first part of the work addresses the sliding wear behavior of such coatings, whereas the relevant cavitation erosion studies are reported in the second part.

2. EXPERIMENTAL PROCEDURE

2.1 Materials and deposition

Five series of coatings, each one containing different fractions of the cermet component, were deposited onto AISI 304 stainless steel substrates (60×70×5 coupons) via HVOF thermal spraying. The feedstock powders were prepared by premixing in a ball mill two commercially available powders: a self-fluxing NiCrFeBSiC metallic and a WC-Co/Cr cermet one, purchased from Sulzer Metco, Winterthur Switzerland. Their characteristics are listed in Table 1.

Table 1. Characteristics of the feedstock powders employed, as provided by the supplier.

	Feedstock powder No 1	Feedstock powder No 2
Commercial name:	Diamalloy 2001	WOKA 3651
Nature:	Metallic	Cermet
Chemical Composition:	Ni, 17 % Cr, 4 % Fe, 4 % Si, 3,5 % B, 1 % C	WC, 10 % Co, 4 % Cr
Particle size range:	-45 + 15 μm	-53 + 20 μm
Morphology:	Globular, produced via condensation of steam (gas atomisation)	Globular (agglomerated sintered)

The cermet powder fraction in the five mixtures was 0, 25, 50, 75 and 100 %vol. to obtain coatings with the corresponding nominal compositions. The respective coatings are denoted herein as: 0 % WC-Co/Cr (metallic), 25 % WC-Co/Cr, 50 % WC-Co/Cr and 75 % WC-Co/Cr (composite), and 100 % WC-Co/Cr (cermet). Deposition was realized in the facilities of the company Pyrogenesis, Greece. The values of the spraying parameters were in-house optimized to ensure minimal WC decarburization.

Prior to deposition the substrate surface was sand-blasted to remove surface impurities and achieve surface roughness promoting the mechanical anchorage of the coatings onto the metallic substrate.

The average roughness (R_α) of the as-sprayed coatings was measured 8.0±0.5 μm. Since this value is relatively high, the specimens prior to tribological testing were polished to a roughness level of 1.0±0.2 μm.

2.2 Tribological testing and examination techniques

Sliding friction tests were performed in dry air (25%RH, 20 °C) using a ball-on-disc apparatus (Centre Suiss d' Electronique et de Microtechnique, CSEM). A silicon nitride (Si_3N_4) ball of 6 mm in diameter was used as a counterbody. Specimens of all series were tested under 10 N normal load, 200 $mm.s^{-1}$ sliding speed and for a total sliding distance of 10000 m. Silicon nitride was employed since, an alumina ball, used as counterbody in preliminary tests under the same conditions, was worn much faster than the systems under study to be employed as a reference material. During testing the friction coefficient was recorded as a function of sliding distance. The total wear volume was calculated by measuring with a stylus profilometer (Taylor–Hobson) the track cross-sectional area at ten different locations along the wear track and by multiplying the average track area by the circumference of the slide cycle.

The crystallographic phases of the coatings were identified by X-ray diffraction (XRD). XRD patterns were recorded with a Siemens D500 diffractometer, with auto-divergent slit and graphite monochromator, using CuKa radiation and a scanning speed of 2 $°.min^{-1}$. Vickers microhardness measurements were carried out on a SHIMADZU-M apparatus, applying a load of 0.3 kg. The measurements were performed on

cross-sections of the coatings to provide an estimate of the effect of the cermet addition on the coatings mechanical properties. Twenty such measurements were performed for each composition. Microstructure characterisations, as well as detailed analysis of the worn surfaces were conducted with the aid of an FEI XL40 SFEG scanning electron microscope (SEM) equipped with an energy dispersive X-ray spectrometry (EDS) detector for elemental analysis. Prior to microhardness measurements and SEM observations of the cross-sections of the worn specimens, special attention was paid for the metallographic preparation, in order to avoid insertion of secondary defects. First, the specimens were carefully sectioned using diamond and SiC cutting wheels, for the cermet coating and the metallic substrate, respectively. The cross-sections were cold mounted under vacuum using an impregnation resin suitable for the observation of open pores and cracks.

3. RESULTS AND DISCUSSION

3.1 Microstructure evaluation

The average coating thickness values were estimated by microscopy observations of cross-sections and were found ~210, ~350 and ~280 μm, for the metallic, cermet and composite coatings, respectively. In Fig. 1 such representative cross-sections of the five coating compositions are shown, under the same, low magnification to facilitate direct comparison. All the coatings appeared to have dense structures, low porosity and being macro-crack free. Moreover, in all cases the coatings' inner surface followed closely the free surface of the sand-blasted substrate, filling any gaps and achieving thus good adhesion to the substrate by anchorage mechanism [36]. Indeed, adhesion measurements performed according to ASTM C633-13 specification: "Standard Test Method for Adhesion or Cohesion Strength of Thermal Spray Coatings", demonstrated adhesion strength values higher than 75 MPa. This is a threshold value beyond which adhesion for ceramic thermal sprayed coatings onto stainless steel substrates is considered to be very good [37]. The random solidification of the arriving molten particles onto the already solidified ones induced an erratic orientation of the surface splats, which resulted in the relevantly high (8.0 ± 0.5 μm) average roughness measured on the as-sprayed coating.

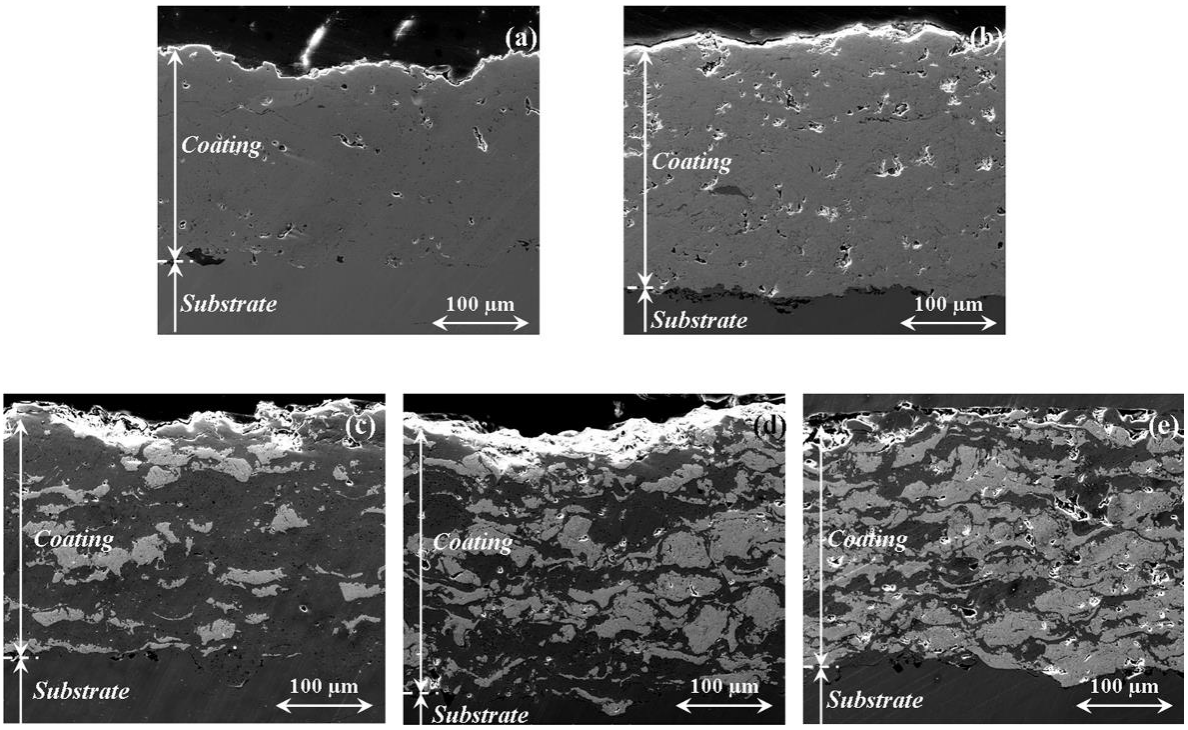

Fig. 1. SEM micrographs of characteristic cross sections of the coatings examined: (a) 0 % WC-Co/Cr, (b) 100 % WC-Co/Cr, (c) 25WC-Co/Cr, (d) 50 WC-Co/Cr and (e) 75WC-Co/Cr.

Typical XRD spectra of the five coatings are compared in Fig. 2, where a total of five crystalline phases can be distinguished. The phases detected with XRD were identified and correlated to microstucture features of the coatings. Such typical features can be distinguished in representative SEM photographs of the 0 %, 100 % and 50 % WC-Co/Cr coatings, shown in Figs. 3a, 3b and 3c, respectively.

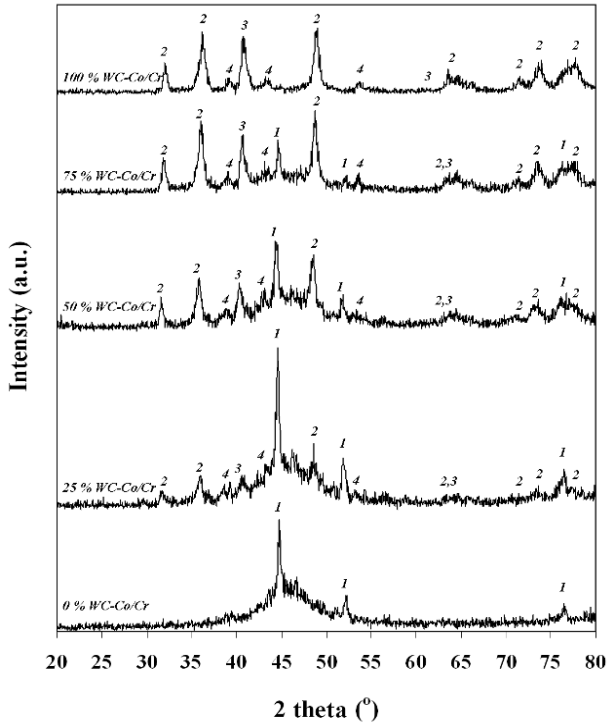

Fig. 2. X-ray diffraction spectra of the composite coatings examined. Labels correspond to the locus of main reference peaks of: fcc (Ni) 1, WC 2, W_2C 3 and W 4.

The predominant phase detected in the 0% WC-Co/Cr coating (bottom spectrum), marked as 1, corresponded to face-centered cubic Ni solid solution (γ-Ni). The characteristic broadening of the diffraction peak around 2θ of 44° is indicative of partial amorphization or nano-crystalline phases within the coating, attributed to the inherently high splat cooling rate of the HVOF process [20,29,33]. Other distinct crystalline phases among the elements Cr, Fe, Si, B and C, contained in the metallic feedstock, were not detected. However, from the SEM observations and the relevant local EDS elemental microanalysis (Fig. 3a), it is evident that the coating consisted of a γ-Ni (light grey color), within which Cr-rich precipitates (dark grey color) were highly and homogeneously dispersed. The latter were of spherical-like morphology, having a diameter less than 2 μm. Similar microstructure was observed in previous microstructural studies on HVOF sprayed Ni-50Cr coatings [31].

In the case of the 100 % WC-Co/Cr coating (top spectrum, Fig. 2), the major phases identified were those of WC and W_2C, marked as 3 and 4 respectively, whilst W, marked as 5, was also present in minor quantity. The existence of W_2C and W has been frequently observed in such coatings, attributed to in-flight decarburization of WC. This phenomenon has been extensively discussed in the relevant literature [2,16-24] and various decarburization mechanisms have been proposed, such as thermal-only decomposition, reaction with oxygen, or carbide dissolution within the metallic binder [17]. The extent of decarburization has been correlated to the ratio of partial pressures of CO/CO_2 in the spraying atmosphere and the granulometry of the feedstock powder [7].

The respective microstructure shown in Fig. 3b, was characterized in the one hand by sporadic elliptic interlamellar micro-porosity at the splat-to-splat boundaries and in the other hand by two distinct regions of approximately equal fraction but of different chemical composition, as shown in the respective EDS spectra. Spherical-like particles, of 2.5 μm maximum size, consisting of tungsten carbides (denoted by only the W peak, since C is below the detection limit and does not appear in the EDS spectra), were highly dispersed within a Co-Cr-W matrix. These observations are in agreement with the top spectrum in Fig. 2.

As expected, the composite coatings' spectra exhibited all five phases described above (Fig. 2). Microscopic observation of composite coatings revealed similar microstructure features for all the cermet fractions. Distinct metallic and cermet splats can be clearly distinguished in Fig. 3c that corresponds to the 50 % WC-Co/Cr coating.

The area spanned by all microhardness measurements performed on cross-sections of the coatings is shown in Fig. 4. Even though the effective microhardness values exhibited increased scattering with increasing cermet fraction, the general trend was that the average effective microhardness also increased with increasing cermet fraction. The minimum values

for the three composite coatings were approximately constant and equal to ~720 HV0.3, coinciding with that of the pure metallic coating (0 % WC-Co/Cr). In contrast, their maximum microhardness values increased almost linearly with cermet content from 890 to 1200 HV0.3, whilst the maximum value measured was 1420 HV0.3, corresponding to 100 % WC-Co/Cr. A similar behavior has been observed in a previous study, where a linear decrease of hardness with increasing metal binder content was reported for various monolithic cermet systems. In that work, hardness values for monolithic WC-Co cermets were found to decrease from 1450 to 880 HV10 with an increase of the metal binder from 10 to 32 % [38].

The model of Lee and Gurland [39], commonly applied to cermets, states that higher effective hardness values are achieved with smaller inter-carbide spacing, or, in other words, lower metal binder "mean free path". The term "contiguity" was defined to describe the percentage surface area of a carbide grain in contact with other carbide grains; the higher the contiguity, the higher is the effective hardness. There are several process approaches to alter this "mean free path". For example, in a case of Cr_3C_2–NiCr thermal spray coatings, constraint of the metal binder between the carbides was induced by prolonged post-deposition heat treatment. This process led to precipitation and development of secondary carbides and was found to elevate their effective hardness [40]. In another study concerning WC-12Co coatings [18], the distance between individual WC grains was affected by varying the plasma power.

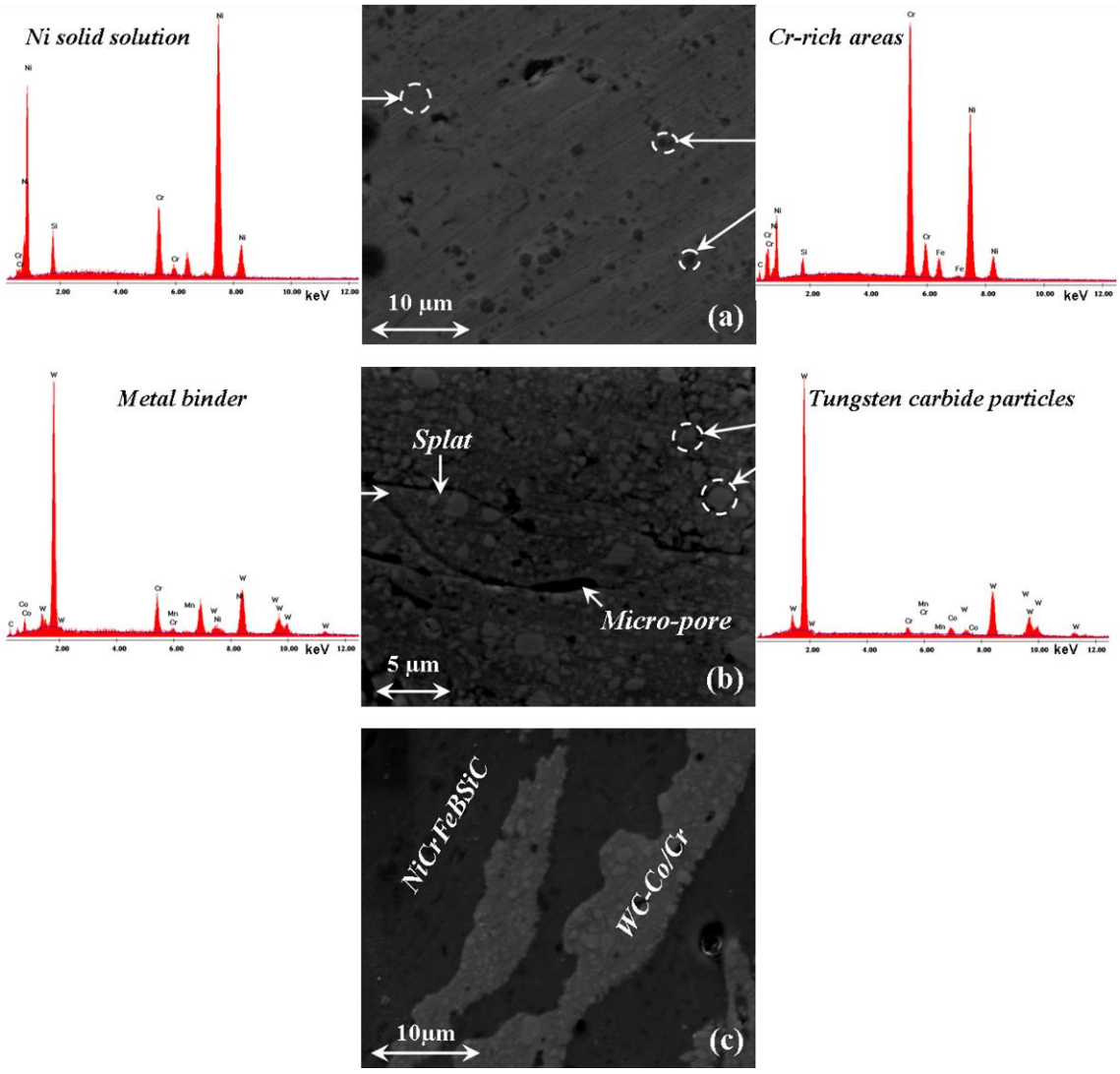

Fig. 3. SEM micrographs and local EDS micro-analysis of representative microstructure features detected in: (a) 0 % WC-Co/Cr, (b) 100 % WC-Co/Cr and (c) 50 % WC-Co/Cr coatings.

The same microhardness trend observed in the present work can be correlated to a similar contiguity of the composite coatings at the splat level. An increase of the cermet fraction increases the probability of a cermet splat to be surrounded by similar hard cermet ones, rather than from softer metallic ones. Therefore, the hardness values measured on the metal binder are higher due to the constraints to its plastic deformation. In the case of cermet fraction decrease, the probability for a cermet splat to be surrounded by metallic ones is higher. The plastic deformation of the metal binder is less constrained, resulting in higher "mean free path" length and, consequently lower hardness values measured.

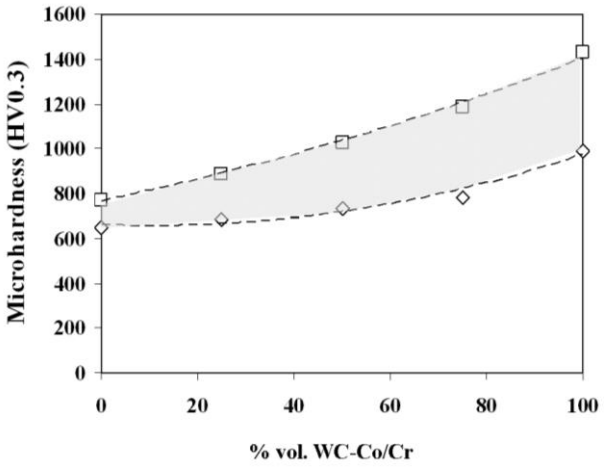

Fig. 4. Effective microhardness range of the coatings, as a function of their cermet content.

3.2 Tribological behavior

The dependence of the steady-state friction coefficient on the cermet fraction is shown in Fig. 5a. Its values increased from 0.48 in the case of the 0 % WC-Co/Cr coatings, up to 0.68 in the case of 50 % WC-Co/Cr coatings. For higher cermet content values it decreased again down to a minimum value of 0.44 for 100 % WC-Co/Cr coatings. Such a behavior is indicative of differences in the wear mechanisms, strongly dependent on the cermet fraction, to be discussed in detail in the next section.

The total volume loss after 10000 m sliding versus the cermet fraction is shown in Fig. 5b. The almost linear reduction of the volume loss resulted in a respective linear decrease of the wear coefficient values from 2.96×10^{-5} to 3.62×10^{-6} $mm^3N^{-1}m^{-1}$, as calculated from the Lancaster formula (1) below [38]:

$$k = \frac{V}{s \times F} \quad (1)$$

Where: V, the wear volume in mm^3
s, the sliding distance in m
F, the normal load applied in N

Similar trends of a linear decrease of the wear loss with the WC content in the metallic matrix were observed in block-on-disc testing of powder metallurgy monolithic cermets [38], as well as of powder welding composite coatings [41]. Even though the two studies above examined different carbide fraction ranges from the present study, the similarity of the general trends observed advocates for a generic mechanism of the carbides intervention on the wear micro-mechanisms taking place during sliding friction of mixed carbide/ metallic matrix systems.

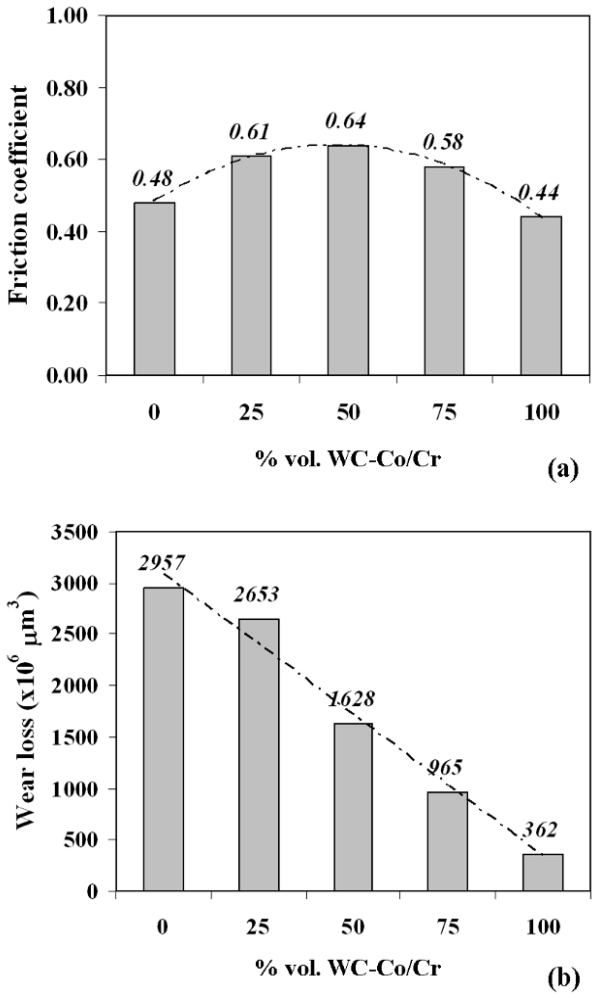

Fig. 5. Sliding friction characteristics of the coatings, as a function of their cermet content: (a) Mean friction coefficient and (b) Mean wear volume loss.

Table 2. Representative literature values of sliding friction and wear coefficients for WC-based HVOF cermet coatings.

Composition	Sliding testing/ Counterbody/ Conditions	Friction coefficient	Wear	Reference
WC-12Co	Ball-on-disc/ Sintered WC-Co ball/ 15 N, 0.10 m,s^{-1}, 1000 m	0.28	Non-measurable	[7]
WC-12Co	Pin-on-disc/ Hardened steel disc/ 49 N, 1 m.s^{-1}, 4500 m	0.52	30×10^{-6} mm^3/N.m	[15]
WC-30Ni	Ball-on-disc/ Si_3N_4 ball/ 1,7 kg (16.67 N), 30 mm.s^{-1}, 54 m 300°C	0.35	9.42×10^{-3} mm^3 (1.05×10^{-5} mm^3/N.m)	[12]
WC-10Co-4Cr	Pin-on-disc/ Hardened steel/ 30 N, 0.5 m.s^{-1}, 2500 m	0.51 (conventional powder) 0.33 (nano-size powder)	3×10^{-3} gr 2.2×10^{-3} gr	[8]
WC-10Co-4Cr	Ball-on-disc/ Sintered Al_2O_3/ 25 ˚C, 55%RH/ 400 °C/ 600 °C/ 750 °C 10 N, 0.1 m.s^{-1}, 5000 m	0.44/ 0.78/ 0.52/ 0.64	$6x10^{-8}$/ 7×10^{-8}/ 5×10^{-7}/ 1.5×10^{-4} mm^3/N.m	[22]
WC-10Co-4Cr	Ball-on-disc/ Sintered Al_2O_3/ 70 N, 0.9 m.s^{-1}, 1500 m, 10 % RH	0.45	~95 mm^3 (9.05×10^{-4} mm^3/N.m)	[26]
WC-10Co-4Cr	Pin-on-disc/ Pin WC–6 wt% Co / 30 N, 0.10 m.s^{-1}, 25 °C, 50 % RH	0.30	$3.6x10^{-9}$ mm^3/N.m	[42]
WC-10Co-4Cr	Ball-on-disc/ Si_3N_4 ball 10 N, 0.20 m.s^{-1}, 10000 m	0.44	0.362 mm^3, 3.62×10^{-6} mm^3/N.m	This study

The values of friction and wear coefficient determined in this study for the cermet coating (100 % WC-Co-Cr) are listed in Table 2, together with relevant values reported in the recent literature for representative WC-based HVOF cermet coatings and sliding conditions. The friction coefficient is in the same range with most literature values; these are of the same order irrespective of the tribosystem examined. The wear coefficient is of the same order of magnitude with some of the respective values reported, which are anyway characterized by high discrepancies among them, since the volume removal is strongly dependent on the particular testing conditions (counterbody, normal load, sliding distance).

3.3 Wear mechanisms

A typical SEM photograph spanning the whole width of the wear track for the 0 % WC-Co/Cr coating is shown in Fig. 6a. Within that, areas of different morphological characteristics, denoted as (b), (c), (d) and (e) were identified, delineating the activation of distinct wear micro-mechanisms on the same contact area. Higher SEM magnifications on these areas (also shown in Figs. 6 b-e, respectively) were employed to further elucidate micro-phenomena associated to coating removal. Polishing lines along the sliding direction, together with micro-ploughing traces are clearly seen in Fig. 6b. These are indicative of typical abrasion wear, encountered when an elastic ceramic body (Si_3N_4) is sliding against an elastoplastic metallic surface (0% WC-Co/Cr coating). The examined metallic surface exhibited local oxidation areas verified via EDS micro-analysis as shown in Fig. 6c, indicative of the activation of a tribo-oxidation mechanism. SEM observations at the single-splat-scale level revealed that the coating was worn out in the one hand through the normally expected material removal via debris creation and in the other hand by inter- as well as intra-splat micro-cracking, as shown in Fig. 6d. A final "snapshot" of the intervention of micro-cracking at the wear mechanism is presented in Fig. 6e, where the propagation of cracks perpendicular to the sliding direction led to eventual splat exfoliation and consequently to relatively increased wear rates, as also observed previously [29].

In the case of 100 % WC-Co/Cr coating, magnification at the level of typical splats having remained in the wear track (Fig. 7) demonstrated that material removal occurred via steady-state wear debris creation, generated by micro-fragmentation of the metal binder matrix of surface splats. Intra-splat cracks propagating through the matrix and deflected at the carbide particle boundaries were clearly

seen, whereas entire-splat exfoliation areas were not observed.

The wear micro-mechanisms observed in the case of composite coatings are a synergy of those of the two extreme cases of 0 % and 100 % WC-Co/Cr coatings. Their contribution to the final macroscopic wear is correlated not only to the fraction of the two individual phases, but to the nature of contact between the surface exposed to wear and its underlayer as well. Indeed, the co-spraying of metallic and cermet particles resulted in the random deposition of metallic and cermet splats both along each particular layer, as well as across the whole coating thickness. In other words, the activation of a particular wear mechanism depends not only on the nature of the particular wear surface splats (metallic or cermet), but also on the nature of the sub-surface splats directly underneath them. For example, the wear micro-mechanisms of a surface cermet splat deposited onto a pre-deposited metallic one (Fig. 8a), exhibited a steady-state wear though debris creation and fragmentation of the metallic matrix of the cermet splat. The decohesion of the metallic matrix led to pull-out of the tungsten carbides, as also observed previously [28], that remained on the worn surface during testing (Fig. 8b).

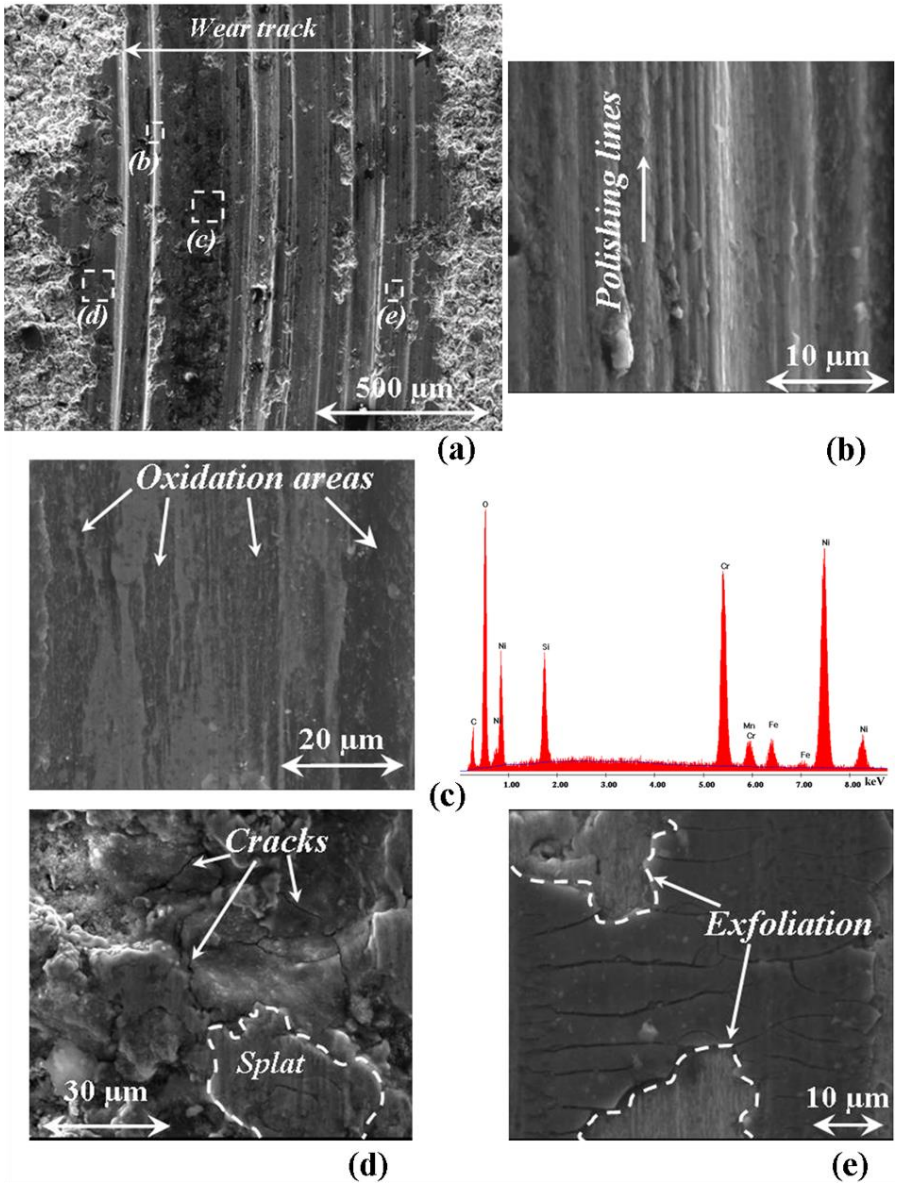

Fig. 6. SEM top-view micrographs of the worn surface of the metallic coating and relevant wear micro-mechanisms detected: (a) Typical view of the entire wear track width; (b) Polishing accompanied by micro-ploughing; (c) Localized oxidation areas, verified by EDS microanalysis; (d) Inter- and intra-splat micro-cracking; (e) Micro-cracks perpendicular to the sliding direction, resulting in entire splat exfoliation.

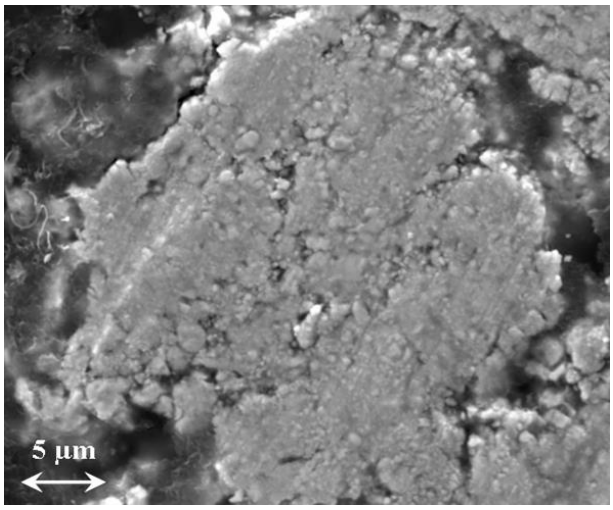

Fig. 7. SEM top-view micrograph of the cermet coating's worn surface, demonstrating micro-fragmentation of a single splat.

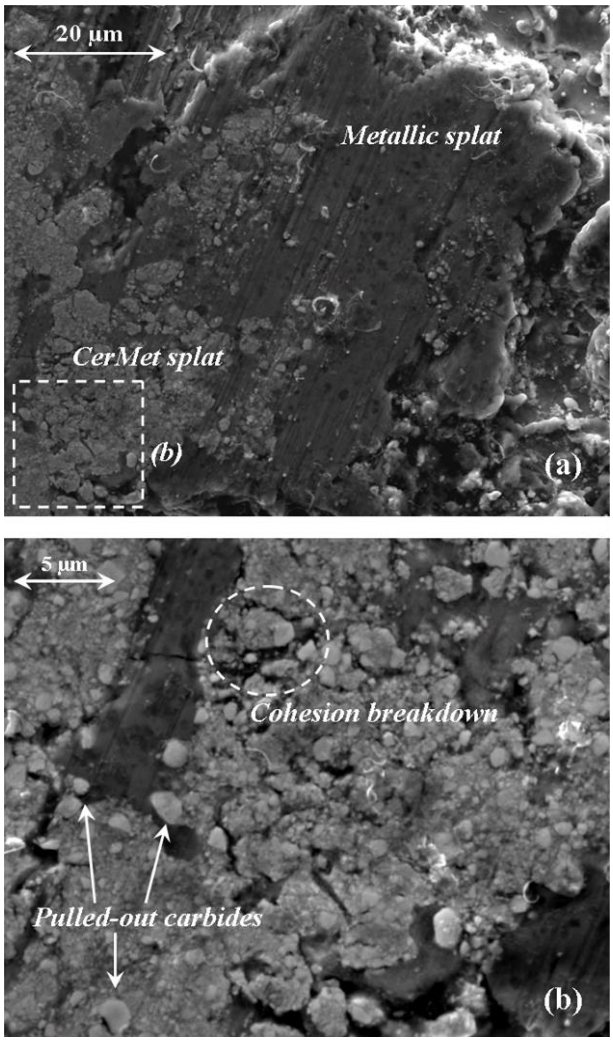

Fig. 8. SEM top-view micrographs of a detail of the worn surface of the 75 % WC-Co/Cr composite coating indicating: (a) Wear of a cermet splat revealing the underlying metallic one; (b) Magnification of relevant marked area in (a), showing decohesion of the metal binder and pull-out of tungsten carbides.

In another case, depicted in Fig. 9a, both metallic and cermet splats were simultaneously exposed to sliding wear. The wear track area magnified in Fig. 9b, was characterized by the development of cracks primarily along the cermet/ metallic splat interfaces. The void observed at the centre of the photograph most likely occured due to carbide pull-out discussed above. In areas like the one magnified in Fig. 9c, where the cermet phase has been removed, cermet wear debris were trapped within the cavity formed. Finally in the case magnified in Fig. 9d, a metallic surface splat exposed to sliding is shown. Extensive plastic deformation that led to eventual splat in-depth cracking along the sliding direction is clearly observed. Such areas on the whole wear track were located only on protrusions of the coating asperities, where local stresses are concentrated. The development of such cracks can be explained from the sub-splat existence of a rigid cermet layer protrusion that could not be plastically deformed. Thus, progressive wear decrease of the metallic splat thickness culminated to a situation where the tensile stresses developed could not be sustained, resulting in splat cracking.

SEM observations on composite coatings cross-sections revealed subsurface coating damage as well. A cross-section of the specimen, the contact surface of which was presented in Fig. 9, is shown in Fig. 10a for direct comparison. Symmetric cracks were developed at the wear track boundaries at the contact surface and propagated perpendicularly to the coating/ substrate interface, throughout the entire coating thickness (Fig 10b). It is interesting to note that these cracks were not deflected around the boundaries of the cermet splats encountered, but propagated throughout their metallic matrix (Fig. 10c), practically splitting them and resulting in partial decohesion from the underlying metallic layer. This phenomenon was common for all composite coatings, irrespective of their cermet fraction, whereas it was not observed in the case of metallic coatings. However, the extensive fragmentation of the 100 % WC-Co/Cr coatings did not allow its verification there. Even though similar observations have been also recorded in the tribological study of a Detonation-Gun Al_2O_3 coating [43], an underlying mechanism responsible for this behavior cannot be proposed with certainty, at this stage.

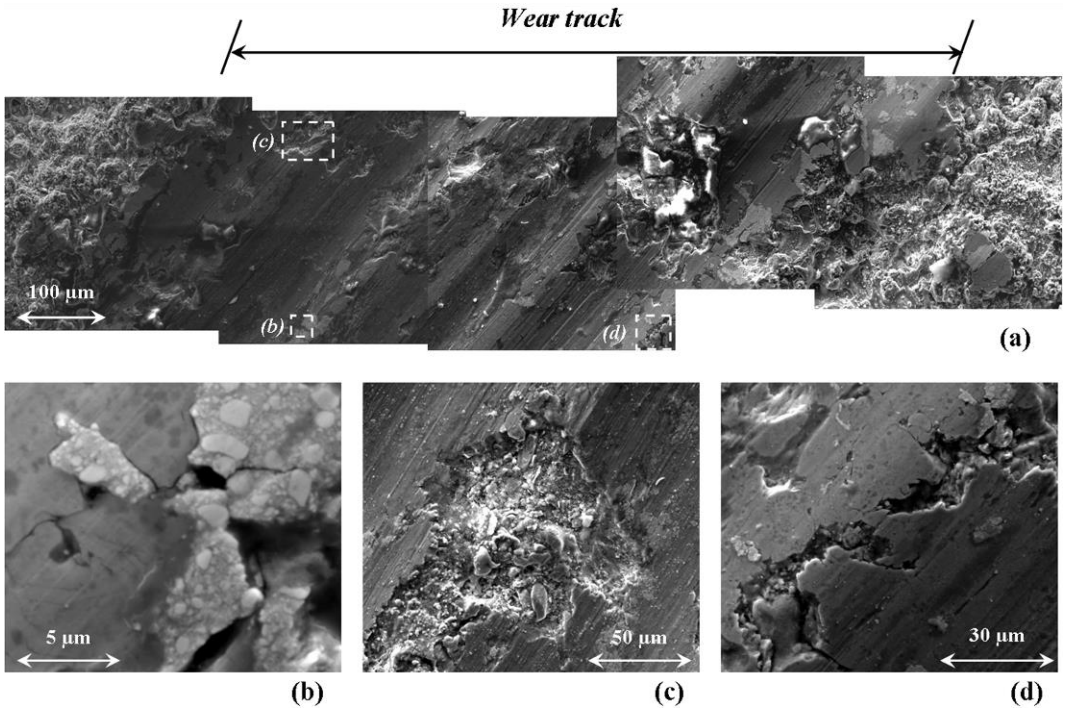

Fig. 9. SEM top-view micrographs of the worn surface of the 50% WC-Co/Cr composite coating and relevant wear micro-mechanisms locally detected: (a) Typical view of the entire wear track width; (b) Characteristic cracks along the interfaces of cermet/ metallic splats both existing at the contact area; (c) Cermet removal and induced debris entrapment; (d) Plastic deformation and tensile cracking along the sliding direction of the metallic phase.

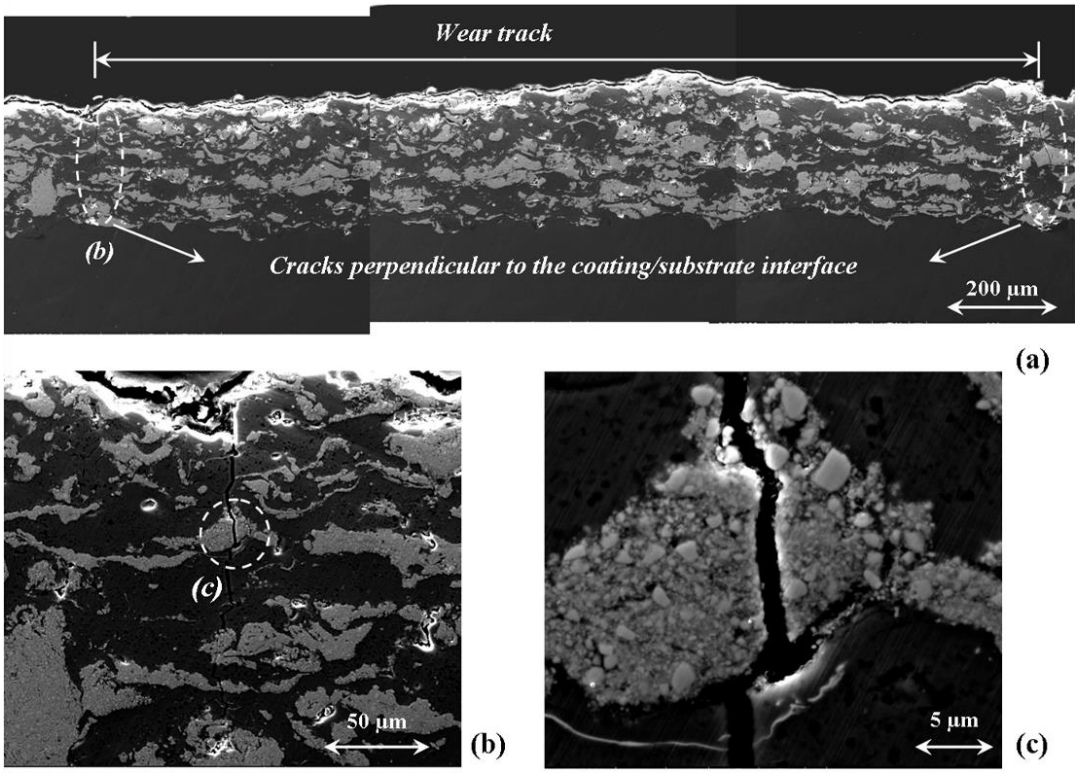

Fig. 10. SEM cross section of micrographs the 50 % WC-Co/Cr composite coating: (a) Typical view of the entire wear track width; (b) Crack propagation at the boundaries of the wear track, perpendicular to the coating/ substrate interface; (c) Magnification of relevant marked area in (b) indicating trans-cracking of a cermet splat.

An overall possible correlation of the quantitative results from the friction coefficient and wear loss measurements to the qualitative observations of the worn surfaces can be attempted. Even though the wear loss is linearly decreasing with increasing cermet content, the friction coefficient exhibits a maximum value at 50 % cermet content. The lower friction coefficient for the metallic-only coating could be attributed to the formation of an oxide tribo-layer (Fig. 6c) that facilitates sliding, whilst its higher wear rate is relevant to the second main wear micro-mechanism identified on the worn surface, that of entire splat removal. In the other hand, the almost equally low friction coefficient for the cermet-only coating is due to its much higher hardness, whilst its significantly lower wear rate could be associated to the absence of massive material removal via entire splat exfoliation. A possible cause for the different tribological behavior of coatings with intermediate cermet content could be the intervention of wear debris layer remaining on the contact surface and modifying both sliding and wear micro-mechanisms. This debris layer consists of a mixture of metallic and carbide components occurring from the simultaneous wear of both phases. For coatings with composition close to that of the metallic-only one, the carbides particles in the debris act as a third abrasive body, destroying locally the oxide tribo-layer that acts as an in-situ lubricant. The main wear mechanism though, is still that of splat exfoliation. For coatings with composition close to that of the cermet-only one, the debris mixture consists mainly of small size hard carbide particles that in this case act as “micro-bearings”, facilitating sliding. In parallel, the predominant wear mechanism has been shifted to that of splat micro-fragmentation and carbide only pull-out from the metallic binder, inducing much less material removal.

4. CONCLUSION

The sliding wear mechanisms of WC-Co/Cr / NiCrFeBSiC composite coatings developed by HVOF spraying onto AISI 304 stainless steel were studied as a function of the cermet content. Microstructure characterization of the as-deposited coatings mainly revealed partial decomposition of the WC particles and maximum effective hardness values increasing almost linearly with the cermet content. The tribological behaviour was studied in a ball-on-disc apparatus, using a Si_3N_4 ball as counterbody. The average friction coefficient was found to depend strongly on the cermet fraction, exhibiting a maximum value of 0.64, at 50 % WC-Co/Cu content. The wear coefficient values were of the order of 10^{-5} $mm^3.N^{-1}.m^{-1}$, decreasing almost linearly with increasing cermet fraction. Microscopic examinations of the wear tracks were employed to identify the wear mechanisms involved:

- Pure metallic (0 % WC-Co/Cr) coatings were worn out through a synergy of micro-ploughing, micro-cracking and splat exfoliation.
- Micro-cracking of the metal binder at the individual splat scale leading to tungsten carbide particles pull-out, was identified as the dominant material removal mechanism in the case of cermet -only (100 % WC-Co/Cr) coatings.
- Co-spraying of metallic and cermet pre-mixed particles resulting in random deposition of relevant splats along and across the coatings thickness induces local differentiations of the wear micro-mechanisms associated to the nature - metallic or cermet - of both the exposed as well as the sub-surface splats succession. In addition to micro-mechanisms identified on the worn surfaces, in-depth cracks perpendicular to the coating/ substrate interface were observed at the wear track boundaries, resulting in cermet trans-splat fracture.
- Friction coefficient and wear rates variation with respect to the WC-Co/Cr content can be correlated to the material removal micro-mechanisms and the composition of the debris layer remaining at the surface contact during sliding.

To further elucidate the wear behavior of randomly stratified metallic/ cermet thermal sprayed coatings, cavitation erosion tests were performed on the same as-deposited coatings. The relevant wear mechanisms are presented in the second part of this study.

Acknowledgements

The authors would like to acknowledge the help of Dr. C. Agrafiotis, currently at DRL, Cologne, Germany, on the XRD characterizations and of Dr. G. Pantazopoulos, at ELKEME, Athens, Greece, on the specimens' vacuum mounting and the SEM observations, as well as the Post-Graduate programme "Chemistry and Technology of Materials" of University of Ioannina, Greece, for partial financing of this work.

REFERENCES

[1] B. Basu, M. Kalin: *Tribology of ceramics and composites*, Hoboken, New Jersey: John Wiley & Sons, 2011.

[2] A.M.Venter, O.P. Oladijo, V. Luzin, L.A. Cornish, N. Sacks: *Performance characterization of metallic substrates coated by HVOF WC-Co*, Thin Solid Films, Vol. 549, pp. 330-339, 2013.

[3] M. Heydarzadeh Sohi, F. Ghadami: *Comparative tribological study of air plasma sprayed WC-12%Co coating versus conventional hard chromium electrodeposit*, Tribology International, Vol. 43, pp. 882-886, 2010.

[4] A.K. Basak, P. Matteazzi, M. Vardavoulias, J.-P. Celis: *Corrosion-wear behaviour of thermal sprayed nanostructured FeCu/WC-Co coatings*, Wear, Vol. 261, No. 9, pp. 1042-1050, 2006.

[5] A.K. Basak, J.-P. Celis, M. Vardavoulias P. Matteazzi: *Effect of nanostructuring and Al alloying on friction and wear behaviour of thermal sprayed WC-Co coatings*, Surface and Coatings Technology, Vol. 206, No. 16, pp. 3508-3516, 2012.

[6] A.K. Basak, J.-P. Celis, P. Ponthiaux, F. Wenger, M. Vardavoulias P. Matteazzi: *Effect of nanostructuring and Al alloying on corrosion behaviour of thermal sprayed WC-Co coatings*, Materials Science and Engineering A, Vol. 558 pp. 377-385, 2012.

[7] J.M. Guilemany, S. Dosta, J.R. Miguel: *The enhancement of the properties of WC-Co HVOF coatings through the use of nanostructured and microstructured feedstock powders*, Surface and Coatings Technology, Vol. 201, No. 3-4, pp. 1180-1190, 2006.

[8] L. Thakur, N. Arora: *Sliding and abrasive wear behavior of WC-CoCr coatings with different carbide sizes*, Journal of Materials Engineering and Performance, Vol. 22, No. 2, pp. 574-583, 2013.

[9] R.J.K. Wood: *Tribology of thermal sprayed WC-Co coatings*, International Journal of Refractory Metals and Hard Materials, Vol. 28, No. 1, pp. 82-94, 2010.

[10] S. Wirojanupatump, P.H. Shipway, D.G. McCartney: *The influence of HVOF powder feedstock characteristics on the abrasive wear behaviour of Cr_xC_y-NiCr coatings*, Wear, Vol. 249, No. 9, pp. 829-837, 2001.

[11] J. Stokes, L. Looney: *HVOF system definition to maximise the thickness of formed components*, Surface and Coatings Technology, Vol. 148, No. 1, pp. 18-24, 2001.

[12] S.L. Liu, X.P. Zheng: *Microstructure and properties of AC-HVAF sprayed Ni60/WC composite coating*, Journal of Alloys and Compounds, Vol. 480, No. 2, pp. 254-258, 2009.

[13] Q. Wang, S. Zhang, Y. Cheng, J. Xiang, X. Zhao, G. Yang: *Wear and corrosion performance of WC-10Co4Cr coatings deposited by different HVOF and HVAF spraying processes*, Surface and Coatings Technology, Vol. 218, pp. 127-136, 2013.

[14] B.L. Zha, S.L. Qiao, D.Y. Huang, W. He, Z.H. Zha, X.B. Li: *Study of properties of nanostructured and conventional WC-12Co coatings deposited by HVO/AF*, Advanced Materials Research, Vol. 709, pp. 166-171, 2013.

[15] H.S. Sidhu, B.S. Sidhu, S. Prakash: *Wear characteristics of Cr_3C_2-NiCr and WC-Co coatings deposited by LPG fueled HVOF*, Tribology International, Vol. 43, No. 5-6, pp. 887-890, 2010.

[16] C. Verdon, A. Karimi, J.-L. Martin: *A study of high velocity oxy-fuel thermally sprayed tungsten carbide based coatings. Part 1: Microstructures*, Materials Science and Engineering A, Vol. 246, No. 1-2, pp. 11-24, 1998.

[17] M.F. Morks, Y. Gao, N.F. Fahim, F.U. Yingqing, M.A. Shoeib: *Influence of binder materials on the properties of low power plasma sprayed cermet coatings*, Surface and Coatings Technology, Vol. 199, No. 1, pp. 66-71, 2005.

[18] M.F. Morks, Y. Gao, N.F.Fahim, F.U. Yingqing: *Microstructure and hardness properties of cermet coating sprayed by low power plasma*, Materials Letters, Vol. 60, No. 8, pp. 1049-1053, 2006.

[19] T. Sahraoui, N.-E. Fenineche, G. Montavon, C. Coddet: *Structure and wear behaviour of HVOF sprayed Cr_3C_2-NiCr and WC-Co coatings*, Materials and Design, Vol. 24, No. 5, pp. 309-313, 2003.

[20] M. Xie, S. Zhang, M. Li: *Comparative investigation on HVOF sprayed carbide-based coatings*, Applied Surface Science, Vol. 273, pp. 799-805, 2013.

[21] T. Sahraoui, S. Guessasma, M. Ali Jeridane, M. Hadji: *HVOF sprayed WC-Co coatings: Microstructure, mechanical properties and friction moment prediction*, Materials and Design, Vol. 31, No. 3, pp. 1431-1437, 2010.

[22] G. Bolelli, L.-M. Berger, M. Bonetti, L. Lusvarghi: *Comparative study of the dry sliding wear behaviour of HVOF-sprayed WC-(W,Cr)$_2$C-Ni and WC-CoCr hardmetal coatings*, Wear, Vol. 309, No. 1-2, pp. 96-111, 2014.

[23] C.W. Lee, J.H. Han, J. Yoon, M.C. Shin, S.I. Kwun: *A study on powder mixing for high fracture toughness and wear resistance of WC-Co-Cr coatings sprayed by HVOF*, Surface and Coatings Technology, Vol. 204, No. 14, pp. 2223-2229, 2010.

[24] H. Liao, B. Normand, C. Coddet: *Influence of coating microstructure on the abrasive wear resistance of WC/Co cermet coatings*, Surface and Coatings Technology, Vol. 124, No. 2-3, pp. 235-242, 2000.

[25] W. Fang, T.Y. Cho, J.H. Yoon, K.O. Song, S.K. Hur, S.J. Youn, H.G. Chun: *Processing optimization, surface properties and wear behavior of HVOF spraying WC-CrC-Ni coating*, Journal of Materials Processing Technology, Vol. 209, No. 7, pp. 3561-3567, 2009.

[26] S. Hong, Y. Wu, B. Wang, Y. Zheng, W. Gao, G. Li: *High-velocity oxygen-fuel spray parameter optimization of nanostructured WC-10Co-4Cr coatings and sliding wear behavior of the optimized coating*, Materials and Design, Vol. 55 pp. 286-291, 2014.

[27] J.A. Picas, E. Rupérez, M. Punset, A. Forn: *Influence of HVOF spraying parameters on the corrosion resistance of WC-CoCr coatings in strong acidic environment*, Surface and Coatings Technology, Vol. 225, pp. 47-57, 2013.

[28] K. Kumari, K. Anand, M. Bellacci, M. Giannozzi: *Effect of microstructure on abrasive wear behavior of thermally sprayed WC-10Co-4Cr coatings*, Wear, Vol. 268, No. 11-12, pp. 1309-1319, 2010.

[29] P. Sharma, J.D. Majumdar: *Microstructural characterization and properties evaluation of Ni-based hardfaced coating on AISI 304 stainless steel by high velocity oxyfuel coating technique*, Metallurgical and Materials Transactions A, Vol. 44, No. 1, pp. 372-380, 2013.

[30] N.F. Ak, C. Tekmen, I. Ozdemir, H.S. Soykan, E. Celik: *NiCr coatings on stainless steel by HVOF technique*, Surface and Coatings Technology, Vol. 174-175, pp. 1070-1073, 2003.

[31] J. Saaedi, T.W. Coyle, S. Mirdamadi, H. Arabi, J. Mostaghimi: *Phase formation in a Ni-50Cr HVOF coating*, Surface and Coatings Technology, Vol 202, No. 24, pp. 5804-5811, 2008.

[32] J. Saaedi, H. Arabi, T.W. Coyle, S. Mirdamadi, , H. Ghorbani: *Corrosion resistance of Ni-50Cr HVOF coatings on 310S alloy substrates in a metal dusting atmosphere*, Materials and Corrosion, Vol. 62, No. 9, pp. 823-835, 2011.

[33] S. Hong, Y. Wu, G. Li, B. Wang, W. Gao, G. Ying: *Microstructural characteristics of high-velocity oxygen-fuel (HVOF) sprayed nickel-based alloy coating*, Journal of Alloys and Compounds, Vol. 581, pp. 398-403, 2013.

[34] G. Bolelli, V. Cannillo, L. Lusvarghi, R. Rosa, A. Valarezo, W.B. Choi, R. Dey, C. Weyant, S. Sampath: *Functionally graded WC–Co/NiAl HVOF coatings for damage tolerance, wear and corrosion protection*, Surface and Coatings Technology, Vol. 206, No. 8-9, pp. 2585–2601, 2012.

[35] D. Aussavy, S. Costil, O. El Kedim, G. Montavon, A-F Bonnot: *Metal matrix composite coatings manufactured by thermal spraying: Influence of the powder preparation on the coating properties*, Journal of Thermal Spray Technology, Vol. 23, No. 1-2, pp. 190-196, 2014.

[36] D. Pantelis, P. Psyllaki, N. Alexopoulos: *Tribological behaviour of plasma-sprayed Al_2O_3 coatings under severe wear conditions*, Wear, Vol. 237, No. 2, pp. 197-204, 2000.

[37] G. Rosa, P. Psyllaki, R. Oltra, T. Montesin, C. Coddet, S. Costil: *Laser ultrasonic testing for estimation of adhesion of Al_2O_3 plasma sprayed coatings*, Surface Engineering, Vol. 17, No. 4, pp. 332-338, 2001.

[38] J. Pirso, M. Viljus, K. Juhani, S. Letunovitš: *Two-body dry abrasive wear of cermets*, Wear, Vol. 266, No. 1-2, pp. 21-29, 2009.

[39] H.C. Lee, J. Gurland: *Hardness and deformation of cemented tungsten carbide*, Materials Science and Engineering, Vol. 33, No. 1, pp. 125-133, 1978.

[40] S. Matthews, M. Hyland, B James: *Microhardness variation in relation to carbide development in heat treated Cr_3C_2–NiCr thermal spray coatings*, Acta Materialia, Vol. 51, No. 14, pp. 4267-4277, 2003.

[41] N.Y. Sari, M. Yilmaz: *Improvement of wear resistance of wire drawing rolls with Cr-Ni-B-Si + WC thermal spraying powders*, Surface and Coatings Technology, Vol. 202, pp. 3136-3141, 2008.

[42] J.A. Picas, Y. Xiong, M. Punset, L. Ajdelsztajn, A. Forn, J.M. Schoenung: *Microstructure and wear resistance of WC-Co by three consolidation processing techniques*, Journal of Refractory Metals and Hard Materials, Vol. 27, No. 2, pp. 344-349, 2009.

[43] P. Psyllaki, M. Jeandin, D. Pantelis: *Microstructure and wear mechanisms of thermal-sprayed alumina coatings*, Materials Letters, Vol. 47, No. 1-2, pp. 77-82, 2001.